

Article

A Decision-Support Informatics Platform for Minimally Invasive Aortic Valve Replacement

Katia Capellini ^{1,*}, Vincenzo Positano ¹, Michele Murzi ², Pier Andrea Farneti ², Giovanni Concistrè ², Luigi Landini ³ and Simona Celi ^{1,*}

¹ BioCardioLab, Department of Bioengineering, Fondazione CNR-Regione Toscana “G. Monasterio”, 54100 Massa, Italy; positano@ftgm.it

² Department of Adult Cardiac Surgery, Fondazione CNR-Regione Toscana “G. Monasterio”, 54100 Massa, Italy; michele.murzi@ftgm.it (M.M.); farneti@ftgm.it (P.A.F.); concistre@ftgm.it (G.C.)

³ Department of Information Engineering, University of Pisa, 56122 Pisa, Italy; llandini@ftgm.it

* Correspondence: kcapellini@ftgm.it (K.C.); s.celi@ftgm.it (S.C.)

Abstract: Minimally invasive aortic valve replacement is performed by mini-sternotomy (MS) or less invasive right anterior mini-thoracotomy (RT). The possibility of adopting RT is assessed by anatomical criteria derived from manual 2D image analysis. We developed a semi-automatic tool (RT-PLAN) to assess the criteria of RT, extract other parameters of surgical interest and generate a view of the anatomical region in a 3D space. Twenty-five 3D CT images from a dataset were retrospectively evaluated. The methodology starts with segmentation to reconstruct 3D surface models of the aorta and anterior rib cage. Secondly, the RT criteria and geometric information from these models are automatically and quantitatively evaluated. A comparison is made between the values of the parameters measured by the standard manual 2D procedure and our tool. The RT-PLAN procedure was feasible in all cases. Strong agreement was found between RT-PLAN and the standard manual 2D procedure. There was no difference between the RT-PLAN and the standard procedure when selecting patients for the RT technique. The tool developed is able to effectively perform the assessment of the RT criteria, with the addition of a realistic visualisation of the surgical field through virtual reality technology.

Keywords: aortic valve replacement; minimally invasive technique; 3D models; image processing; rib cage



Citation: Capellini, K.; Positano, V.; Murzi, M.; Farneti, P.A.; Concistrè, G.; Landini, L.; Celi, S. A Decision-Support Informatics Platform for Minimally Invasive Aortic Valve Replacement. *Electronics* **2022**, *11*, 1902. <https://doi.org/10.3390/electronics11121902>

Academic Editor: Gemma Piella

Received: 26 May 2022

Accepted: 15 June 2022

Published: 17 June 2022

Publisher's Note: MDPI stays neutral with regard to jurisdictional claims in published maps and institutional affiliations.



Copyright: © 2022 by the authors. Licensee MDPI, Basel, Switzerland. This article is an open access article distributed under the terms and conditions of the Creative Commons Attribution (CC BY) license (<https://creativecommons.org/licenses/by/4.0/>).

1. Introduction

Aortic valve disease (AVD) has become one of the most common causes of cardiovascular disease in the developed world, causing significant morbidity and mortality [1,2]. The high prevalence of AVD and its increase with age indicate the growing burden of these diseases. AVD represents a serious and growing public health problem for which adequate resources are always needed to improve research in diagnosis and treatment [3,4]. Surgical aortic valve replacement (AVR) by total median sternotomy is the gold standard in the treatment of symptomatic AVD. Several minimally invasive approaches for AVR have been proposed to minimise surgical trauma, and their use continues to increase [5–8]. Minimally invasive aortic valve replacement (MIAVR) is the standard approach in many centres and has been shown to improve surgical outcomes [9–11]. The surgical approach for MIAVR is usually via a mini-sternotomy (MS), which provides a 6–10 cm vertical midline skin incision, which performs a partial J sternotomy from the third to fifth intercostal space or a V-shaped MS at the second intercostal space (2nd IS) or third intercostal space (3rd IS) [12]. The MS technique has the advantage of the reducing ventilation time and length of hospital stay [13,14]. Another newer and less invasive approach for MIAVR is the right anterior mini-thoracotomy technique (RT), which is performed through a 5–7 cm lateral skin incision at the second IS or third IS level starting from the edge of the sternum without

rib resection [15,16]. RT has shown excellent clinical outcomes in MIAVR procedures, such as a lower incidence of postoperative atrial fibrillation, reduced blood transfusion and earlier extubation [17–19]. In addition, the preservation of the sternum by RT would reduce postoperative pain, respiratory function is improved and the smaller pericardial incision, together with the lack of manipulation of the right atrium for venous drainage, would minimise the inflammatory response. With all these aspects, the RT approach could be associated with lower postoperative morbidities, shorter hospital stay and less rehabilitation than MS [20–22]. The RT approach is excluded for patients with a history of cardiac surgery, previous right-sided pleuritis and aortic root dilatation [23]. RT approach is considered feasible if specific conditions are met regarding the position and distance of the aorta from the sternum and the angle of the aortic plane in relation to the patient's axis. With the increasing use of preoperative imaging [24–26], the RT feasibility could be assessed by image analysis. Approximately 200 surgical procedures (including MS and RT) are performed at our centre each year. To determine RT feasibility, patients should undergo a computed tomography (CT) scan to evaluate the anatomical relationships among the ISs, sternum, ascending aorta and aortic valve. The following criteria define these geometric features: (i) at the level of the pulmonary artery (PA), the ascending aorta is rightward (more than half is on the right with respect to the right sternal border); (ii) the distance between the posterior ascending aorta and the sternum (asD) does not exceed 10 cm; (iii) the α angle (angle between the angle midline and the inclination of the ascending aorta) should be $>45^\circ$ [16]. If all these conditions are not met, the MS procedure could be considered as an alternative technique for MIAVR [20]. The RT criteria as well as the morphological indices are currently assessed by manual measurements, analysing slice-by-slice volumetric sets of axial CT images. Therefore, the relative positions in real 3D space are not taken into account and the procedure for evaluating the criteria is operator dependent. The aim of this study was to develop a semi-automatic 3D image analysis routine for right thoracotomy (RT-PLAN) that is able to extract all required parameters from 3D CT images. The RT-PLAN tool can also provide a 3D view of the aorta, sternum, ribs and their relative spatial relationships as additional features. The developed tool was tested and validated on the CT datasets of 25 patients scheduled for MIAVR.

2. Materials and Methods

2.1. Image Analysis

The images of 25 patients (14 females and 11 males with an average age of 75 years) scheduled for MIAVR were retrospectively analysed. All subjects signed an informed consent form. Preoperative CT images were acquired with a 320-detector scanner (Toshiba Aquilion One, Toshiba, Japan) during one deep inspiratory breath-hold and were characterised by a pixel size of 0.625 mm, a resolution of 512×512 and a slice thickness of 0.5 mm. According to clinical protocols, all datasets were acquired after the intravenous injection of contrast medium. Manual slice-by-slice 2D measurements taken and recorded by an experienced surgeon during preoperative planning served as reference. The reference measurements were performed with the software OsiriX MD v.10.0.1 (Pixmeo, Geneva, Switzerland). The workflow of the RT-PLAN procedure consists of two main steps. The first step involves the creation of 3D models of the aorta and anterior rib cage (aRC). The second step involves the geometric analysis of the aorta and aRC models in 3D space to evaluate the RT criteria and estimate additional morphological indices.

2.2. Aorta and aRC 3D Models Reconstruction

First, the 3D surface extraction of the aorta and anterior rib cage from the 3D CT datasets and selection of reference points at the level of the PA bifurcation was performed. The ascending aorta was segmented using a region growing algorithm (Figure 1a) and the corresponding 3D surface model and mesh were generated from the obtained mask (Figure 1b). Basically, the region growing algorithm starts with a seeded region and includes the neighbouring pixels based on a predefined criterion to determine whether they should

also be considered as part of the object to be segmented. The selected pixels were added to the region and the process is repeated to enlarge the region. OsiriX software was used for this task, which selects the seed on the contrast agent inside the blood vessel. Meshmixer software (Autodesk Inc., Toronto, ON, Canada) was used to improve the quality of the 3D mesh of the ascending aorta to obtain a model that can be used in the second step of the RT-PLAN method. In particular, the segmentation was smoothed by morphological closure, which also fills any possible small holes [27]. The centreline of the aorta was also extracted. The second part of the workflow is dedicated to aRC segmentation. Due to the presence of cartilage components in the anterior rib tract, the aRC region is characterised by a wide range of greyscales, making use of the region growing algorithm for aRC reconstruction (RG-aRC) unsuitable due to excessive processing time. To overcome this limitation, a faster alternative and semi-automatic approach (ROI-aRC) for generating the aRC surface model was defined and implemented. The reconstruction of the sternum and the initial part of the first five ribs was performed by developing a specific algorithm based on four main steps. Firstly, for each of the five ribs, four ROIs were drawn in sagittal view (Figure 1c) on the right and on the left of the sternum (Figure 1d). Second, five regions of interest (ROIs) were traced along the sternum in the axial view of the CT dataset (Figure 1d,e). In the third step, the ROIs of the ribs and sternum were converted into polylines and different lofts were generated to connect adjacent polylines to reconstruct each rib tract and the sternum (Figure 1d). Finally, all created parts of the rib cage were joined together to obtain the final aRC surface model in STL format (Figure 1f). The centrelines of all ribs and the sternum were also extracted. The delineation of the ROIs and the creation of the 3D surface model were performed using the FreeCAD programme (www.freecadweb.org), which is integrated with Python 3.6 software by implementing a custom routine.

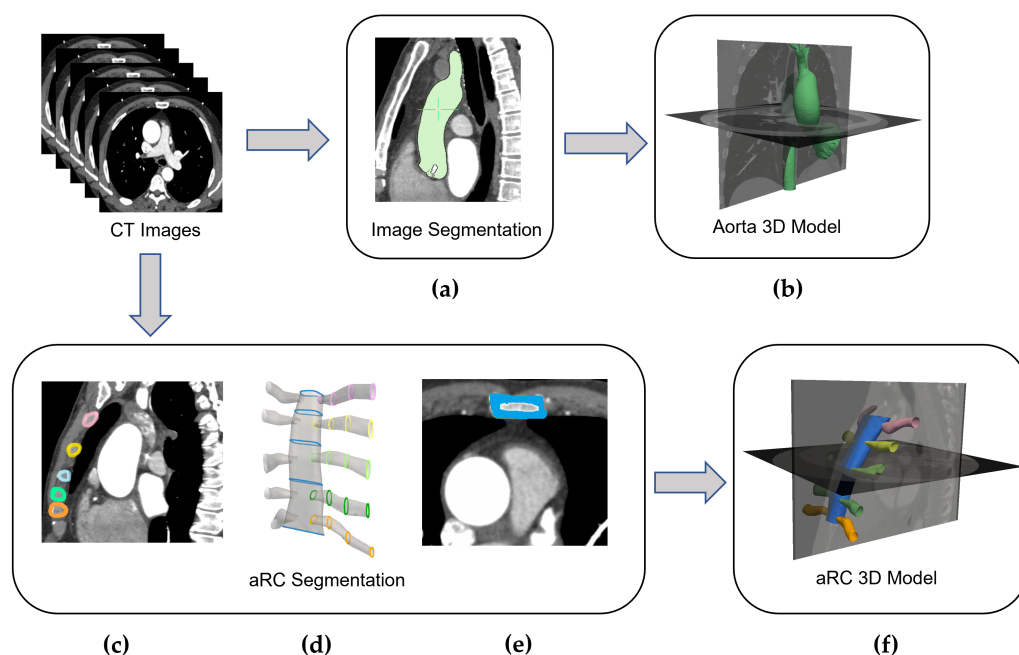


Figure 1. Procedure for aorta and aRC 3D models reconstruction.

2.3. RT Inclusion Criteria Evaluation and Geometric Parameters Extraction

The second step of RT-PLAN allows the automatic assessment of the RT criteria and the extraction of the geometric parameters of surgical interest from the 3D surface model of the ascending aorta [28] and the aRC. The rightward placement of the aorta in relation to the sternum (first RT criterion, Figure 2a) is verified by comparing the 3D coordinates of the right sternal border and the 3D coordinates of the ascending aortic centreline at the level of the pulmonary bifurcation. For the assessment of the second RT criterion, planes

perpendicular to the sternum were automatically extracted based on the sternal centreline and the intersection with the surface of the aorta was calculated, allowing the calculation of the asD index (Figure 2b). Finally, the α angle (third RT criterion) was calculated starting from the direction of the aortic centerline in the valve area with respect to the foot-to-head (FH) direction (Figure 2c). The reference measurements on the CT images are also shown in Figure 2a–c for comparison.

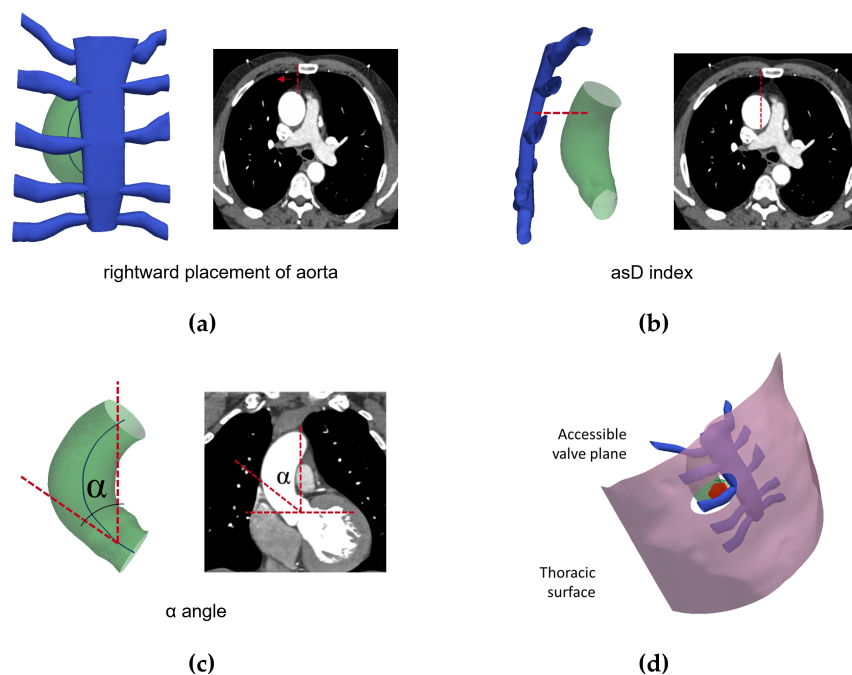


Figure 2. RT inclusion criteria evaluation (a–c) and a patient-specific virtual “planning/surgery” (d).

Other geometric parameters useful for surgical technique such as the maximum diameter of the sino-tubular junction (SJD), the perimeter of sino-tubular junction section (SJP) and the width of the sternum (SW) were also extracted. To identify the sino-tubular junction, a specific routine was implemented to analyse the shape of the aortic cross-sections based on the circularity shape factor ($4\pi A/P^2$), where A and P are the cross-sectional area and perimeter, respectively. The sino-tubular junction is identified as a loss of circularity with respect to the aortic cross-sections. Other parameters of interest are the width of the 2nd IS and 3rd IS and the distance between the incision position and the centre of the section of the sino-tubular junction (IV).

To facilitate an easier understanding of the relative spatial relationships between 3D surface models and to promote virtual analysis during preoperative planning, the RT-PLAN provides a visualising 3D interface. In particular, the procedure allowed the qualitative 3D visualisation of the position of the ascending aorta in relation to the sternum by defining a sagittal plane intersecting with the right sternal border and a coronal plane at 10 cm from the sternal surface.

An important aspect of the RT surgical technique is the characterisation of the field of view through which the aortic valve can be accessed, both in terms of the visible valve area and the angle of view. Finally, the RT-PLAN could provide a patient-specific virtual “planning/surgery” consisting of a 3D reconstruction of the surgical incision and an interactive assessment of the possible viewing directions of the surgeon during the procedure. In addition, the tool provides the maximum visible area of the sino-tubular junction and the viewing direction closest to the perpendicular view of the valve plane, taking into account the surgeon’s distance from the aortic valve along with the surgical incision position (Figure 2d). The second step of the RT-PLAN was implemented in Python and VTK/VMTK languages.

2.4. Validation and Statistical Analysis

The accuracy of the aRC model reconstructed using the ROI-aRC approach was assessed by estimating the error in model reconstruction (E_{rec}). The E_{rec} value was calculated as the distance of the mesh vertices between the aRC model obtained with the RG-aRC technique and the aRC model constructed with the implemented approach in a subset of 5 patients. Validation of the RT criteria and the 3D extracted geometric parameters (SJD, SJP, SW) was performed by comparing the RT-PLAN results with the recorded manual 2D measurements performed by an expert during preoperative planning using the Osirix MD software. The assessment of the RT criteria using the manual 2D approach consists of the visual assessment of the correct placement of the aorta in relation to the right sternal border (Figure 2a), the measurement of the asD in the axial view (Figure 2b) and the calculation of the α angle in the coronal view (Figure 2c). To assess the statistical significance of the differences found, the paired t-test was used based on the features extracted by both methods. A p value of 0.01 was considered significant. Agreement between RT-PLAN and the manual methods was assessed using Bland–Altman analysis and Pearson’s correlation analysis.

3. Results

The validity of RT-PLAN developed tool was demonstrated since the extraction of all features of interest was possible for each analysed subject.

3.1. Segmentation and 3D Model Reconstruction

The surface models of the ascending aorta and the aRC portion were successfully reconstructed for all datasets. The generation of the surface model of the aorta took 10.1 ± 2.3 min. The reconstruction of the aRC surface model by our approach required 9.2 ± 3.4 min. Note that operator intervention is only required for the phase of ROI tracing in any plane, which took most of the time. For comparison, the aRC surface model built using the RG-aRC approach could even take several hours. Figure 3a shows the bar plot of the E_{rec} for a representative case. The mean distance between the two models was 1.40 mm and ranged from 7.14×10^{-5} mm to 7.15 mm; a spatial map of the E_{rec} distribution on the sternum-ribs surface model is shown in Figure 3b. Analysis of the five patients showed a mean E_{rec} value of 1.38 ± 0.26 mm.

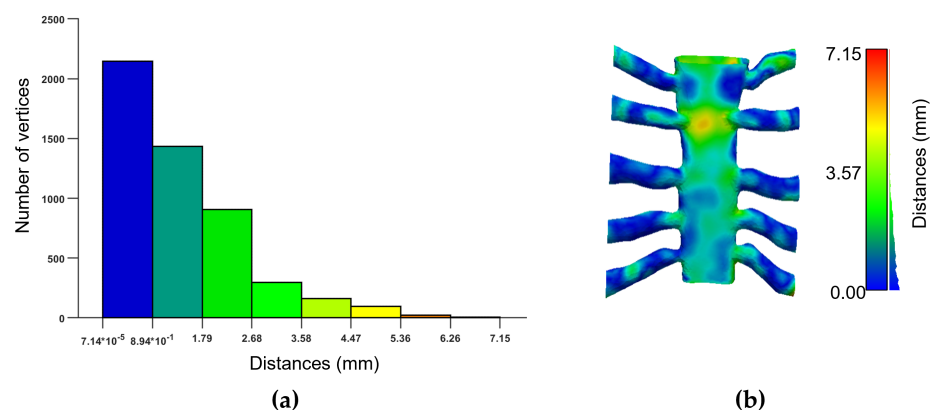


Figure 3. Bar plot of the E_{rec} for a representative case. Only 121 vertices show a distance of more than 4.47 mm on a total of 5070 mesh points and of these, only 26 present a distance ranging between 5.36 and 7.15 mm (a). The spatial localisation of E_{rec} to visualise which regions present the minimum and maximum differences between the two approaches for aRC reconstruction (b).

3.2. RT Inclusion Criteria Evaluation and Geometric Parameters Extraction

The RT criteria estimation was feasible in all cases and the aforementioned morphological features were extracted for all 3D models. The results of the t-test analysis were reported in Table 1. A non-significant difference between the measures performed by an expert operator in 2D space and measures extracted with an RT-PLAN tool was found for

RT criteria, SJP and SW parameters; the SJD revealed a significant difference between the two methodologies. Pearson’s correlation coefficients between the manual measurements and RT-PLAN for RT inclusion criteria, SJD, SJP and SW evaluation ranged from 0.947 (SW) to 0.999 (asD).

Table 1. Comparison between the reference method and the RT-PLAN tool for direct and derived measures.

Parameter	RT-PLAN	Reference
asD (cm)	7.50 ± 1.10	7.47 ± 1.10
α (°)	48.16 ± 10.2	47.76 ± 9.64
SJP (cm)	9.57 ± 1.46	9.55 ± 1.38
SJD (cm)	3.15 ± 0.48 ¹	3.08 ± 0.47
SW (cm)	2.82 ± 0.43	2.48 ± 0.44

¹ $p < 0.001$.

The Bland–Altman analysis showed no significant bias for both observers for the direct (α angle and asD) (Figure 4a,b) and derived measures (SJP, SJD, SW) (Figure 4c–e).

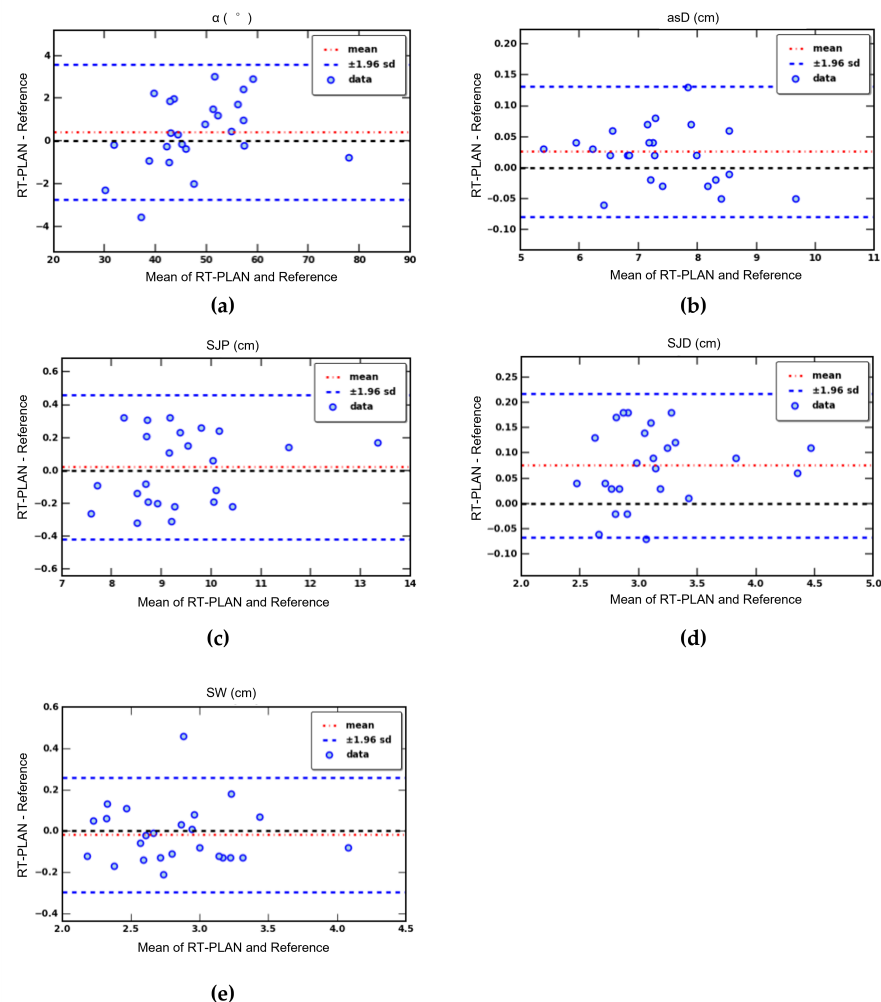


Figure 4. Bland–Altman plot for α angle (a), asD (b), SJP (c), SJD (d) and SW (e) parameters.

The reference procedure and RT-PLAN method were able to classify the patients studied in the same way on the basis of each RT criteria. In particular, the ascending aorta was found rightward in relation to the sternum in the same 10 subjects with both the RT-PLAN and the reference method; asD was found <10 cm in 24 subjects (RT-PLAN: 7.38 ± 0.95 cm, reference 7.36 ± 0.96 cm) and in only one case did it result in ≥ 10 cm (RT-PLAN: 10.39 cm,

reference 10.22 cm); the α angle was $\geq 45^\circ$ for 14 subjects (RT-PLAN: $54.91^\circ \pm 7.87^\circ$, reference $54.09^\circ \pm 7.2^\circ$) and it was $< 45^\circ$ for 11 subjects (RT-PLAN: $39.58^\circ \pm 5.10^\circ$, reference $39.71^\circ \pm 4.22^\circ$). The RT inclusion criteria were met in the same six patients using both methods. A statistical analysis of asD, α angle, SJP, SJD and SW for subjects eligible and ineligible for RT is presented in Table 2. In addition, the indices extracted only with the RT-PLAN tool (2nd IS width, 3rd IS width and IV) are given. No significant difference was found between RT and no RT subjects.

Table 2. Indices values for all parameters examined for both subjects suitable and unsuitable for RT.

Parameters	Patients RT (n = 6)		Patients NO RT (n = 19)	
	Reference	RT-PLAN	Reference	RT-PLAN
<i>Rightward aorta (%)</i>	100	100	21	21
<i>asD (cm)</i>	7.55 ± 0.49	7.57 ± 0.48	7.40 ± 1.24	7.43 ± 1.25
<i>α ($^\circ$)</i>	51.54 ± 3.98	52.35 ± 4.16	46.79 ± 10.80	46.96 ± 11.43
<i>SJP (cm)</i>	9.27 ± 0.65	9.28 ± 0.73	9.53 ± 1.51	9.55 ± 1.59
<i>SJD (cm)</i>	2.97 ± 0.20	3.06 ± 0.23	3.08 ± 0.51	3.14 ± 0.52
<i>SW (cm)</i>	2.64 ± 0.44	2.63 ± 0.46	2.89 ± 0.42	2.87 ± 0.41
<i>2nd IS width (cm)</i>	-	2.15 ± 0.35	-	2.07 ± 0.55
<i>3rd IS width (cm)</i>	-	1.90 ± 0.25	-	1.64 ± 0.38
<i>IV (cm)</i>	-	8.02 ± 0.53	-	8.35 ± 0.80

4. Discussion

MIAVR resulted to be a valid technique with many clinical advantages over traditional surgical approaches for AVR. Among these MIAVR strategies, the RT technique has shown the best clinical outcomes in terms of postoperative pain, short recovery time and cosmetic results. The feasibility of the RT procedure is ensured if certain criteria related to the anatomical location of the aorta and sternum are met. Until now, RT criteria have been assessed by extracting manual measurements from axial CT images, not taking into account the relative positions in real 3D space and the dependence on the expert who performs the analysis. In this work, we developed a novel method to assess the RT criteria starting from a 3D model reconstruction of the anterior rib cage and ascending aorta. Our system was developed to extract the RT required measurements in 3D anatomical space in a semi-automatic way and to allow the assessment of additional morphological features. In this way, manual and operator-dependent 2D image analysis currently used in preoperative planning [20] were transferred to a 3D space to reduce operator-induced variability and improve patient selection.

The aorta segmentation was performed using an established approach [28,29]. As the segmentation of the ribs is a difficult task [30,31], a dedicated tool was developed to generate a 3D surface model of the sternum and the starting tracts of the first five ribs in a fast, semi-automatic and reproducible way. The model created with our approach ensures a good level of confidence (Figure 3a). The working time required for the RT-PLAN procedure was approximately 20 min, which is compatible with clinical practise, with a significant reduction in the required process time and manual interaction. The non-significant difference between the reference and RT-PLAN procedures for asD, α angle, SJP and SW assessment confirms that the two techniques are interchangeable (Table 1). The significant difference in the SJD measurement results from the fact that RT-PLAN extracts the actual maximum diameter of the sino-tubular junction, whereas the manual method traces the diameter manually on axial views, leading to possible systematic underestimations. The reference method and the RT-PLAN method were able to classify the examined patients in the same way based on each of the RT criteria. The proposed approach allowed clinical decision making about patients scheduled for MIAVR procedures to be supported in a rapid and reproducible manner. The analysis of real patient data confirmed the effectiveness of the method. The proposed methodology allows for the extraction of further interesting parameters through minor modifications of the algorithm. As shown in Figure 2d, the

proposed method enables the realistic visualisation of the surgical field through virtual reality technology. Although the usefulness of this approach was not evaluated in this study, it could add value to MIAVR planning. Despite the encouraging results with clinical evidence, some limitations still remain. A prospective study could be useful to evaluate the improvement in surgical outcome with the proposed RT-PLANE tool compared to the standard manual pre-planning procedure. Although the processing time required by RT-PLAN is a reasonable time for MIAVR pre-planning, it could be further reduced to limit its impact in the clinical setting. The processing time mainly refers to the segmentation phase to obtain aortic and aRC models. Deep learning approaches for medical image processing [32] and segmentation [33] are becoming increasingly common and could be a potential strategy to dramatically increase RT-PLAN time costs through fully automated and fast aRC and aortic reconstruction.

Author Contributions: Conceptualisation, K.C. and S.C.; methodology, K.C. and V.P.; software, K.C.; supervision, V.P., L.L. and S.C.; validation, M.M., P.A.F. and G.C.; visualisation, K.C. and V.P.; writing—original draft, K.C.; writing—review and editing, V.P. and S.C. All authors have read and agreed to the published version of the manuscript.

Funding: This research received no external funding.

Institutional Review Board Statement: The study was conducted according to the guidelines of the Declaration of Helsinki and approved by the Institutional Ethics Committee.

Informed Consent Statement: Informed consent was obtained from all patients involved in the study.

Data Availability Statement: Data are available on request due to privacy restrictions.

Conflicts of Interest: The authors declare no conflict of interest.

References

1. Goldbarg, S.H.; Elmariah, S.; Miller, M.A.; Fuster, V. Insights into degenerative aortic valve disease. *J. Am. Coll. Cardiol.* **2007**, *50*, 1205–1213. [[CrossRef](#)]
2. Hartley, A.; Hammond-Haley, M.; Marshall, D.C.; Saliccioli, J.D.; Malik, I.S.; Khamis, R.Y.; Shalhoub, J. Trends in Mortality From Aortic Stenosis in Europe: 2000–2017. *Front. Cardiovasc. Med.* **2021**, *8*, 748137. [[CrossRef](#)]
3. Carabello, B.A.; Paulus, W.J. Aortic stenosis. *Lancet* **2009**, *373*, 956–966. [[CrossRef](#)]
4. Coffey, S.; Cairns, B.J.; Lung, B. The modern epidemiology of heart valve disease. *Heart* **2016**, *102*, 75–85. [[CrossRef](#)]
5. Cosgrove, D.M.; Sabik, J.F. Minimally invasive approach for aortic valve operations. *Ann. Thorac. Surg.* **1996**, *62*, 596–597. [[CrossRef](#)]
6. Johnston, W.F.; Ailawadi, G. Surgical management of minimally invasive aortic valve operations. *Semin. Cardiothorac. Vasc. Anesth.* **2012**, *16*, 41–51. [[CrossRef](#)] [[PubMed](#)]
7. Nguyen, D.H.; Vo, A.T.; Le, K.M.; Vu, T.T.; Nguyen, T.T.; Vu, T.T.; Pham, C.V.; Truong, B.Q. Minimally Invasive Ozaki procedure in aortic valve disease: The preliminary results. *Innovations* **2018**, *13*, 332–337. [[CrossRef](#)]
8. Di Bacco, L.; Miceli, A.; Glauber, M. Minimally invasive aortic valve surgery. *J. Thorac. Dis.* **2021**, *13*, 1945. [[CrossRef](#)]
9. Merk, D.R.; Lehmann, S.; Holzhey, D.M.; Dohmen, P.; Candolfi, P.; Misfeld, M.; Mohr, F.W.; Borger, M.A. Minimal invasive aortic valve replacement surgery is associated with improved survival: A propensity-matched comparison. *Eur. J. Cardio-Thorac. Surg.* **2015**, *47*, 11–17. [[CrossRef](#)]
10. Glauber, M.; Ferrarini, M.; Miceli, A. Minimally invasive aortic valve surgery: state of the art and future directions. *Ann. Cardiothorac. Surg.* **2015**, *4*, 26.
11. Bruno, P.; Cammertoni, F.; Rosenhek, R.; Mazza, A.; Pavone, N.; Iafrancesco, M.; Nesta, M.; Chiariello, G.A.; Spalletta, C.; Graziano, G.; et al. Improved patient recovery with minimally invasive aortic valve surgery: A propensity-matched study. *Innovations* **2019**, *14*, 419–427. [[CrossRef](#)] [[PubMed](#)]
12. Karimov, J.H.; Santarelli, F.; Murzi, M.; Glauber, M. A technique of an upper V-type ministernotomy in the second intercostal space. *Interact. Cardiovasc. Thorac. Surg.* **2009**, *9*, 1021–1022. [[CrossRef](#)] [[PubMed](#)]
13. Brown, M.L.; McKellar, S.H.; Sundt, T.M.; Schaff, H.V. Ministernotomy versus conventional sternotomy for aortic valve replacement: A systematic review and meta-analysis. *J. Thorac. Cardiovasc. Surg.* **2009**, *137*, 670–679. [[CrossRef](#)] [[PubMed](#)]
14. Khoshbin, E.; Prayaga, S.; Kinsella, J.; Sutherland, F. Mini-sternotomy for aortic valve replacement reduces the length of stay in the cardiac intensive care unit: Meta-analysis of randomised controlled trials. *BMJ Open* **2011**, *1*, e000266. [[CrossRef](#)] [[PubMed](#)]
15. Plass, A.; Scheffel, H.; Alkadhi, H.; Kaufmann, P.; Genoni, M.; Falk, V.; Grünenfelder, J. Aortic valve replacement through a minimally invasive approach: Preoperative planning, surgical technique, and outcome. *Ann. Thorac. Surg.* **2009**, *88*, 1851–1856. [[CrossRef](#)]

16. Miceli, A.; Ferrarini, M.; Glauber, M. Right anterior minithoracotomy for aortic valve replacement. *Ann. Cardiothorac. Surg.* **2015**, *4*, 91.
17. Castrovinci, S.; Emmanuel, S.; Moscarelli, M.; Murana, G.; Caccamo, G.; Bertolino, E.C.; Nasso, G.; Speziale, G.; Fattouch, K. Minimally invasive aortic valve surgery. *J. Geriatr. Cardiol. JGC* **2016**, *13*, 499.
18. Jahangiri, M.; Hussain, A.; Akowuah, E. Minimally invasive surgical aortic valve replacement. *Heart* **2019**, *105*, s10–s15. [[CrossRef](#)]
19. Krishna, R.K.; Santana, O.; Mihos, C.G.; Pineda, A.M.; Weiss, U.K.; Lamelas, J. Minimally invasive aortic valve replacement in octogenarians performed via a right anterior thoracotomy approach. *J. Heart Valve Dis.* **2014**, *23*, 671–674.
20. Miceli, A.; Murzi, M.; Gilmanov, D.; Fugà, R.; Ferrarini, M.; Solinas, M.; Glauber, M. Minimally invasive aortic valve replacement using right minithoracotomy is associated with better outcomes than ministernotomy. *J. Thorac. Cardiovasc. Surg.* **2014**, *148*, 133–137. [[CrossRef](#)]
21. Olds, A.; Saadat, S.; Azzolini, A.; Dombrovskiy, V.; Odronic, K.; Lemaire, A.; Ghaly, A.; Lee, L.Y. Improved operative and recovery times with mini-thoracotomy aortic valve replacement. *J. Cardiothorac. Surg.* **2019**, *14*, 1–7. [[CrossRef](#)] [[PubMed](#)]
22. Seitz, M.; Goldblatt, J.; Paul, E.; Marcus, T.; Larobina, M.; Yap, C.H. Minimally invasive aortic valve replacement via right anterior mini-thoracotomy: Propensity matched initial experience. *Heart Lung Circ.* **2019**, *28*, 320–326. [[CrossRef](#)] [[PubMed](#)]
23. Khan, I.; Smith, J.A.; Trehan, N. Minimally Invasive Right Anterior Mini-Thoracotomy Aortic Valve Replacement. In *Cardiac Surgery Procedures*; IntechOpen: London, UK, 2019.
24. Celi, S.; Martini, N.; Emilio Pastormerlo, L.; Positano, V.; Berti, S. Multimodality imaging for interventional cardiology. *Curr. Pharm. Des.* **2017**, *23*, 3285–3300. [[CrossRef](#)]
25. Daubert, M.A.; Taylor, T.; James, O.; Shaw, L.J.; Douglas, P.S.; Koweek, L. Multimodality cardiac imaging in the 21st century: Evolution, advances and future opportunities for innovation. *Br. J. Radiol.* **2021**, *94*, 20200780. [[CrossRef](#)]
26. Van der Hoeven, B.L.; Schali, M.J.; Delgado, V. Multimodality imaging in interventional cardiology. *Nat. Rev. Cardiol.* **2012**, *9*, 333–346. [[CrossRef](#)]
27. Celi, S.; Gasparotti, E.; Capellini, K.; Vignali, E.; Fanni, B.M.; Ali, L.A.; Cantinotti, M.; Murzi, M.; Berti, S.; Santoro, G.; et al. 3D printing in modern cardiology. *Curr. Pharm. Des.* **2021**, *27*, 1918–1930. [[CrossRef](#)]
28. Capellini, K.; Vignali, E.; Costa, E.; Gasparotti, E.; Biancolini, M.E.; Landini, L.; Positano, V.; Celi, S. Computational fluid dynamic study for aTAA hemodynamics: An integrated image-based and radial basis functions mesh morphing approach. *J. Biomech. Eng.* **2018**, *140*, 111007. [[CrossRef](#)] [[PubMed](#)]
29. Volonghi, P.; Tresoldi, D.; Cadioli, M.; Uselli, A.M.; Ponzini, R.; Morbiducci, U.; Esposito, A.; Rizzo, G. Automatic extraction of three-dimensional thoracic aorta geometric model from phase contrast MRI for morphometric and hemodynamic characterization. *Magn. Reson. Med.* **2016**, *75*, 873–882. [[CrossRef](#)]
30. Staal, J.; van Ginneken, B.; Viergever, M.A. Automatic rib segmentation and labeling in computed tomography scans using a general framework for detection, recognition and segmentation of objects in volumetric data. *Med. Image Anal.* **2007**, *11*, 35–46. [[CrossRef](#)] [[PubMed](#)]
31. Xu, Z.; Bagci, U.; Jonsson, C.; Jain, S.; Mollura, D.J. Efficient ribcage segmentation from CT scans using shape features. In Proceedings of the 2014 36th Annual International Conference of the IEEE Engineering in Medicine and Biology Society, Chicago, IL, USA, 26–30 August 2014; IEEE: Piscataway, NJ, USA, 2014; pp. 2899–2902.
32. Niiya, A.; Murakami, K.; Kobayashi, R.; Sekimoto, A.; Saeki, M.; Toyofuku, K.; Kato, M.; Shinjo, H.; Ito, Y.; Takei, M.; et al. Development of an artificial intelligence-assisted computed tomography diagnosis technology for rib fracture and evaluation of its clinical usefulness. *Sci. Rep.* **2022**, *12*, 8363. [[CrossRef](#)]
33. Fantazzini, A.; Esposito, M.; Finotello, A.; Auricchio, F.; Pane, B.; Basso, C.; Spinella, G.; Conti, M. 3D automatic segmentation of aortic computed tomography angiography combining multi-view 2D convolutional neural networks. *Cardiovasc. Eng. Technol.* **2020**, *11*, 576–586. [[CrossRef](#)] [[PubMed](#)]